BRAIN
A JOURNAL OF NEUROLOGY

Network-level connectivity is a critical feature distinguishing dystonic tremor and essential tremor

Jesse C. DeSimone,[1] Derek B. Archer,[1] David E. Vaillancourt[1,2,3] and Aparna Wagle Shukla[3,4]

Dystonia is a movement disorder characterized by involuntary muscle co-contractions that give rise to disabling movements and postures. A recent expert consensus labelled the incidence of tremor as a core feature of dystonia that can affect body regions both symptomatic and asymptomatic to dystonic features. We are only beginning to understand the neural network-level signatures that relate to clinical features of dystonic tremor. At the same time, clinical features of dystonic tremor can resemble that of essential tremor and present a diagnostic confound for clinicians. Here, we examined network-level functional activation and connectivity in patients with dystonic tremor and essential tremor. The dystonic tremor group included primarily cervical dystonia patients with dystonic head tremor and the majority had additional upper-limb tremor. The experimental paradigm included a precision grip-force task wherein online visual feedback related to force was manipulated across high and low spatial feedback levels. Prior work using this paradigm in essential tremor patients produced exacerbation of grip-force tremor and associated changes in functional activation. As such, we directly compared the effect of visual feedback on grip-force tremor and associated functional network-level activation and connectivity between dystonic tremor and essential tremor patient cohorts to better understand disease-specific mechanisms. Increased visual feedback similarly exacerbated force tremor during the grip-force task in dystonic tremor and essential tremor cohorts. Patients with dystonic tremor and essential tremor were characterized by distinct functional activation abnormalities in cortical regions but not in the cerebellum. We examined seed-based functional connectivity from the sensorimotor cortex, globus pallidus internus, ventral intermediate thalamic nucleus, and dentate nucleus, and observed abnormal functional connectivity networks in dystonic tremor and essential tremor groups relative to controls. However, the effects were far more widespread in the dystonic tremor group as changes in functional connectivity were revealed across cortical, subcortical, and cerebellar regions independent of the seed location. A unique pattern for dystonic tremor included widespread reductions in functional connectivity compared to essential tremor within higher-level cortical, basal ganglia, and cerebellar regions. Importantly, a receiver operating characteristic determined that functional connectivity z-scores were able to classify dystonic tremor and essential tremor with 89% area under the curve, whereas combining functional connectivity with force tremor yielded 94%. These findings point to network-level connectivity as an important feature that differs substantially between dystonic tremor and essential tremor and should be further explored in implementing appropriate diagnostic and therapeutic strategies.

1 Department of Applied Physiology and Kinesiology, University of Florida, Gainesville, FL, USA
2 Department of Biomedical Engineering, University of Florida, Gainesville, FL, USA
3 Department of Neurology, College of Medicine, University of Florida, Gainesville, FL, USA
4 Fixel Center for Neurological Disease, College of Medicine, University of Florida, Gainesville, FL, USA

Correspondence to: Aparna Wagle Shukla
Fixel Center for Neurological Disease, University of Florida, 3450 Hull Road
Gainesville, FL 32607, USA
E-mail: aparna.shukla@neurology.ufl.edu

Introduction

Recently, international experts in dystonia proposed rhythmic tremulous movement as an important feature for characterizing dystonia (Albanese *et al.*, 2013). Clinical studies have reported moderate-to-high incidence of tremor affecting a dystonic body part (dystonic tremor) (Deuschl *et al.*, 1998; Bhatia *et al.*, 2018), especially in cervical dystonia patients who exhibit head and upper-limb tremors that may resemble essential tremor (Deuschl *et al.*, 1997; Pal *et al.*, 2000; Shaikh *et al.*, 2008; Defazio *et al.*, 2013, 2015; Erro *et al.*, 2014). Behavioural studies have attempted to better understand the physiological mechanisms that distinguish dystonic tremor from essential tremor, such as regularity and frequency of tremor oscillations, electromyography, and brainstem excitability (Britton *et al.*, 1994; Münchau *et al.*, 2001; Shaikh *et al.*, 2008, 2015; Nisticò *et al.*, 2012*a*, *b*). What is less clear, and equally critical to the diagnostic and treatment framework, is understanding the brain function deficits associated with dystonic tremor and essential tremor.

Previous functional MRI studies performed mostly in focal dystonia have pointed to abnormal activation and functional connectivity within the sensorimotor cortex, basal ganglia, and cerebellum (Simonyan and Ludlow, 2010, 2012; Delnooz *et al.*, 2013, 2015; Battistella *et al.*, 2016, 2017; Burciu *et al.*, 2017; Filip *et al.*, 2017; Li *et al.*, 2017). These studies have provided no consideration to the specific influence of dystonic tremor on brain function, especially in contrast with essential tremor patients that do not have dystonia. However, a recent study examined brain activation during a speech task in patients with isolated spasmodic dysphonia and spasmodic dysphonia with dystonic voice tremor (SD/DT$_V$) (Kirke *et al.*, 2017). Spasmodic dysphonia and SD/DT$_V$ were associated with activation abnormalities in cortical areas, putamen, and thalamus, whereas middle frontal gyrus and cerebellar activation was reduced in SD/DT$_V$ relative to spasmodic dysphonia (Kirke *et al.*, 2017). This was interpreted to reflect that dystonia and dystonic tremor have distinct neural signatures, and that dystonic tremor is possibly positioned between dystonia and essential tremor based on symptomatology and brain abnormalities common to both conditions. Developing a functional perspective of brain signatures that characterize phenotypically variant forms of dystonic tremor and comparing these signatures to a cohort of essential tremor patients is critical to furthering this assertion.

The primary focus of the current study was to examine changes in blood oxygen level-dependent (BOLD) signal amplitude and functional connectivity that relate to changes in visual feedback during the completion of a grip-force task in patients with dystonic tremor. The dystonic tremor cohort included cervical dystonia patients with dystonic head tremor and the majority had additional upper-limb tremor, as well as one spasmodic dysphonia patient with upper-limb tremor. The rationale in using the force task stems from prior work demonstrating visual feedback-induced exacerbation of grip-force tremor that related to changes in BOLD amplitude in essential tremor (Archer *et al.*, 2018). If changes in visual feedback are similarly robust in exacerbating grip-force tremor in dystonic tremor, this affords an opportunity to test the hypothesis of distinct functional abnormalities that relate to dystonic tremor and essential tremor. First, we used a voxel-wise BOLD amplitude analysis to test the hypothesis that dystonic tremor and essential tremor groups reveal differences in force-related functional activation. Second, we used systematically placed regions of interest in the cortex, basal ganglia, thalamus, and cerebellum to examine functional connectivity based on evidence that the pathways connecting these regions are affected in dystonia (Argyelan *et al.*, 2009; Vo *et al.*, 2015) and essential tremor (Pinto *et al.*, 2003; Raethjen and Deuschl, 2012). Lastly, we performed binary logistic regression with receiver operating characteristic (ROC) analysis and leave-one-out cross-validation (LOOCV) to determine the effectiveness of tremor and functional connectivity in distinguishing between dystonic tremor and essential tremor.

Materials and methods

Participants

This study included 20 patients with dystonic tremor, 18 patients with essential tremor, and 18 healthy individuals who were asymptomatic to tremor. Patients were diagnosed by a movement disorders neurologist using established criteria (Deuschl *et al.*, 1998; Albanese *et al.*, 2013; Bhatia *et al.*, 2018). The dystonic tremor group included 19 cervical dystonia patients with dystonic head tremor and 13 of these had additional upper-limb tremor. There was one spasmodic dysphonia patient who had unilateral dominant upper-limb dystonic tremor. The patients with essential tremor included were part of a previous study (Archer *et al.*, 2018), and we excluded one patient from the essential tremor cohort here because the patient developed dystonia following the original publication. Clinical and demographic characteristics for healthy controls and patient groups are presented in Table 1. All experimental procedures were approved and monitored by the University of Florida Institutional Review Board and

Table 1 Demographic and clinical characteristics

Measure	Group		
	Control	DT	ET
Sample size	18	20	18
Age, years	63.7 ± 7.6	64.7 ± 7.9	65.1 ± 11.8
Sex, male, female	8, 10	5, 15	7, 11
Handedness, right, left	15, 3	17, 3	17, 1
MVC, N	58.9 ± 15.3	51.4 ± 17.4	50.5 ± 16.7
MoCA, total	27.8 ± 1.4	26.3 ± 2.9	27.6 ± 2.8
FTM-TRS, total	0.6 ± 0.9	21.9 ± 12.3	38.2 ± 18.8
FTM-TRS, right upper-limb	0 ± 0	2.3 ± 2.1	4.1 ± 1.6
Disorder duration, years	-	6.5 ± 6.3	23.0 ± 21.0

Count or data represented group means ± standard deviation for demographic and clinical variables for controls, dystonic tremor (DT), and essential tremor (ET). FTM-TRS = Fahn-Talosa-Marin Tremor Rating Scale; MoCA = Montreal Cognitive Assessment.

conducted in ethical accordance with the Declaration of Helsinki. Participants signed consent forms and were in full understanding of the experimental objectives.

MRI set-up and acquisition

MRI data were acquired following overnight withdrawal from tremor medications. In patients with cervical dystonia receiving botulinum toxin, MRI acquisition sessions were scheduled at least 3 months after the last injection. MRI sequences were acquired at 3 T (Philips Achieva) using a 32-channel radiofrequency head coil. Participants were supine in the scanner and performed each task with their right hand resting comfortably to their side. A visual display was projected using a head-coil mounted visor mirror positioned within the field of view at a distance of 35 cm. Cushions reduced head motion.

T_1-weighted anatomical images were acquired using a 3D magnetization-prepared rapid gradient echo (MP-RAGE) sequence with the following parameters: repetition time = 8.2 ms, echo time = 3.7 ms, flip angle = 8°, field of view = 240 mm³, resolution = 1 mm isotropic, 170 continuous axial slices, 0 mm gap. Functional MRI data were acquired using a single-shot gradient echo-planar imaging (EPI) sequence with the following parameters: repetition time = 3000 ms, echo time = 30 ms, flip angle = 90°, field of view = 240 mm³, resolution = 3 mm isotropic, 55 continuous axial slices, 0 mm gap.

Force data acquisition

Force data were acquired using an MRI-compatible fibre-optic force transducer (Neuroimaging Solutions) with 0.025 N resolution housed in a precision grip apparatus. The force data were transmitted via fibre-optic cable to an SM130 Optical Sensing Interrogator (Micron Optics). The interrogator digitized force at 62.5 Hz, which was then converted to Newtons using LabVIEW (National Instruments).

Experimental design

Maximum voluntary contraction (MVC), in Newtons, was obtained prior to imaging. Participants grasped the force transducer with their right hand between the thumb and fingers (Fig. 1A) and were instructed to sustain a maximum force for 3 s. MVC was obtained by computing the mean maximum force amplitude produced across three separate trials interleaved with 60 s rest. Participants were then accustomed to the visual display and force task during a training session outside the MRI environment.

Task functional MRI was acquired across two separate tasks: low and high visual feedback. Each task was performed in a blocked design consisting of alternating rest and force blocks. The duration of each task was 270 s. Each block lasted 30 s, beginning and ending with a rest block. In each task, the visual display consisted of a high contrast black background and two horizontal bars—one fixed white bar representing a target force of 15% MVC, and one dynamic coloured bar that provided online visual feedback of the amount of force produced by the participant. During the rest block, the red bar remained stationary and participants were instructed to passively view the visual display. Transition of the coloured bar from red to green served as a cue for the participant to produce force corresponding to the target bar for 30 s while minimizing force fluctuations (Fig. 1B).

The goal to sustain a steady-state force of 15% MVC remained the same across feedback tasks. Visual feedback gain was altered across tasks (Vaillancourt *et al.*, 2006; Coombes *et al.*, 2010; Archer *et al.*, 2018). We manipulated the optical height of the force amplitude fluctuations provided on the visual display such that in the low visual feedback task, a 1 N difference between colour and target bars was represented by a small spatial dissociation (Fig. 1C). Reducing the visual gain permitted small fluctuations in spatial amplitude of the colour bar, rendering a perceived attenuation of error feedback. In the high visual feedback task, the visual gain was larger such that a 1 N difference between target and colour bars was represented by a larger spatial displacement (Fig. 1D). Thus, the degree of error feedback became augmented by large spatial fluctuations of the colour bar. Exemplar force traces for a single control participant during the high and low feedback tasks are presented in Fig. 1E and representative traces allowing for visual comparison of high, medium, and low levels of force tremor in the dystonic tremor and essential tremor groups are presented in Fig. 2.

Force data statistical analysis

Force data variables for high and low visual feedback including mean force (% MVC), force error [root mean square error: RMSE (N)], spectral power of force between 0–13 Hz (N^2), and force tremor [sum of power of force (N^2) between 4–12 Hz] were computed using MATLAB (Version R2017b). For each participant, the mean of each variable obtained from the middle 25 s of each force block was analysed. Values for mean force, force error, spectral power and force tremor in the low visual feedback task were subtracted from the high visual feedback task, producing high minus low difference scores (mean force$_\Delta$, force error$_\Delta$, spectral power$_\Delta$, force tremor$_\Delta$). We also computed the peak force power (N^2) and peak force frequency (Hz) across each of the force blocks in the low, high, and high minus low (Δ) feedback conditions, and the mean and standard deviation values were computed across the four blocks. All variables were examined for normality (Shapiro-Wilk) and homogeneity of variance (Levene's) and submitted
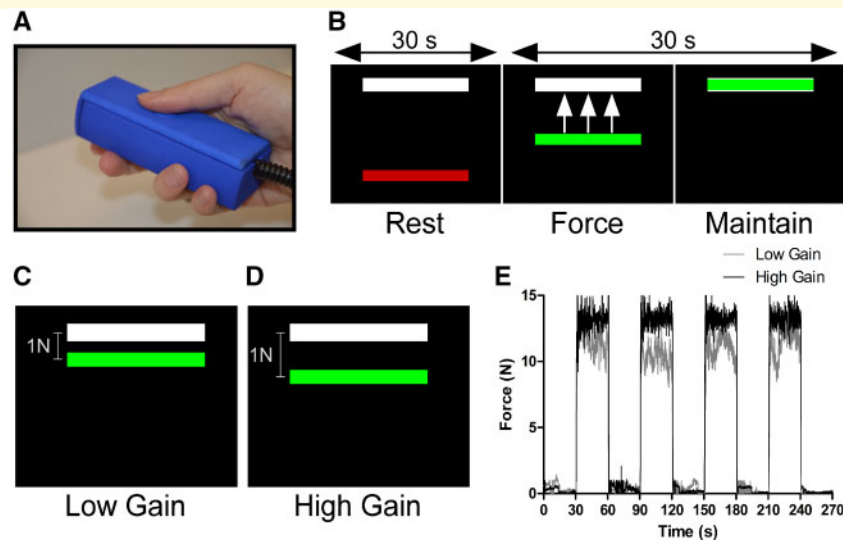
Figure 1 Experimental paradigm. (**A**) The force transducer was held with the right hand between the thumb and fingers and rested comfortably along the side of the body inside the scanner. (**B**) During the 30 s rest block, the visual display consisted of a high contrast black background with white target bar corresponding to 15% MVC and a stationary red colour bar. The transition of the colour bar to green cued participants to produce and maintain 15% MVC for 30 s and provided online visual feedback. (**C**) A 1-N difference between the colour and target bar was represented by a small spatial displacement and visual angle in the low feedback task and (**D**) a large spatial displacement and visual angle in the high feedback task. (**E**) An exemplar force trace for a single control participant during the high (black) and low feedback (grey) tasks showing force fluctuations around 15% MVC.

to either a one-way ANOVA or Kruskal-Wallis test. Significant *F*-statistics were decomposed using either Tukey's honest significant difference test or Dunn's test using rank sums and adjusted for multiple comparisons using the Benjamini-Hochberg false discovery rate (FDR) correction (Benjamini and Hochberg, 1995).

The next goal was to determine whether force tremor could classify dystonic tremor and essential tremor. A binary logistic regression model with forward selection determined the best predictive independent variables and accuracy of the model was tested using an ROC approach and LOOCV. The variables of interest were spectral power$_\Delta$ data within 0–3 and 4–12 Hz and standard deviation of peak force frequency$_\Delta$. The 4–12 Hz bands represent the typical range for entrained motor unit activity producing upper-limb tremor in dystonic tremor and essential tremor (Elble, 1986; Elble *et al.*, 1994; Deuschl and Elble, 2000; Shaikh *et al.*, 2008; Neely *et al.*, 2015) and the 0–3 Hz band can also be elevated in essential tremor (Neely *et al.*, 2015). Standard deviation of peak frequency was selected because tremor frequency can be more irregular across time in dystonic tremor relative to essential tremor (Shaikh *et al.*, 2008; Bove *et al.*, 2018).

Task functional MRI data preprocessing

Preprocessing for functional MRI was carried out using a whole-brain analysis in Analysis of Functional NeuroImages (AFNI: Version 16.0.19) in combination with a cerebellum-optimized pipeline [spatially unbiased infra-tentorial template (SUIT): Diedrichsen, 2006; Diedrichsen *et al.*, 2009] in statistical parametric mapping (SPM8). A combined 1.0-mm motion

exclusion criterion in the *x*-, *y*-, and *z*-planes was used. The following preprocessing steps were performed: removal of the first three functional MRI volumes to account for scanner magnetization equilibrium, slice-timing correction, rigid-body volume registration, co-registration of the functional MRI scan to the T$_1$-weighted anatomical scan, non-linear spatial warping of the functional MRI scan to the MNIavg152 template for the analysis of cerebral data, and cerebellar fine-tuning and normalization to the SUIT template for analysis of cerebellum data. Signal-to-noise ratio was improved by spatial smoothing using a full-width at half-maximum Gaussian kernel of 8 mm and 4 mm for normalized whole-brain and SUIT functional MRI data, respectively.

Task functional MRI statistical analysis

BOLD amplitude data were analysed in the framework of the general linear model. For high and low visual feedback separately, the instantaneous BOLD signal at each voxel and each time-point was scaled by the mean of the BOLD signal across its respective time series. The BOLD signals obtained from the rest and force blocks were modelled using a boxcar regressor convolved with a canonical haemodynamic response function. Non-specific sources of variance including censored head-motion parameters, white matter, and CSF calculated during preprocessing were included in the model as no-interest regressors. Using 3dDeconvolve, the regression was performed across the rest and force blocks to estimate the β-coefficient and its associated *t*-statistic for the BOLD contrast, separately for low and high feedback tasks. BOLD$_\Delta$ statistical maps were generated for each participant by subtracting BOLD statistical
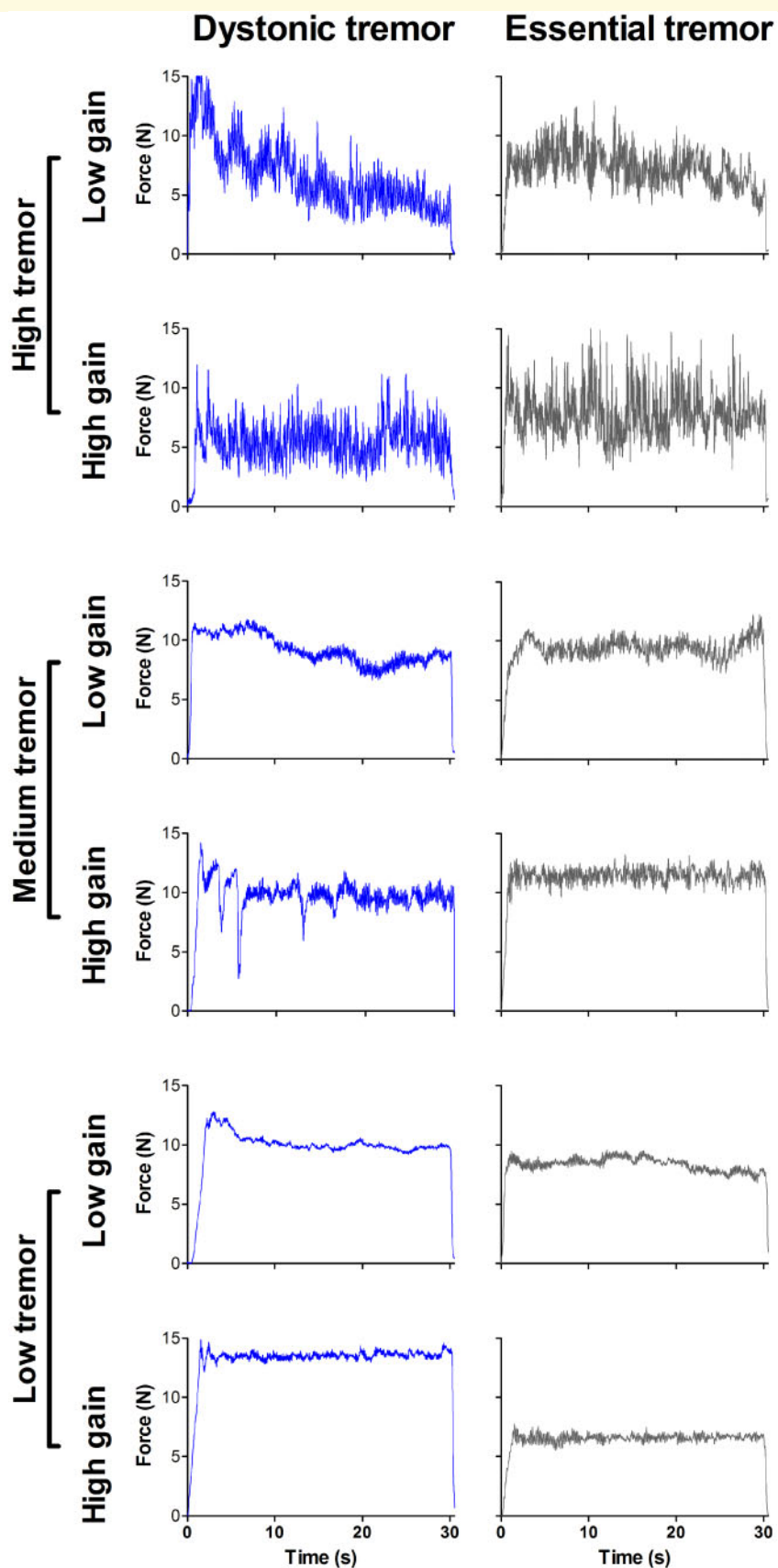
Figure 2 Representative force tremor traces. Force traces for individual dystonic tremor (blue) and essential tremor (grey) patients depicting high (*top*), medium (*middle*), and low (*bottom*) degrees of force tremor for a single 30 s force block in both high and low visual feedback tasks.

maps in the low feedback task from the high feedback task. Between-group comparisons were examined using voxel-wise independent-samples t-tests on the $BOLD_\Delta$ β-coefficients. Consistent with Archer *et al.* (2018), age and BOLD amplitude in the low visual feedback task were included as covariates. Significance level for contrasts was determined using 3dClustSim and set to $P < 0.005$ [$P < 0.05$ familywise error rate (FWER)-corrected] with a minimum cluster size of 243 mm^3 [autocorrelation function (ACF): 0.56, 4.12, 6.88] for whole-brain and 189 mm^3 (ACF: 0.62, 4.19, 4.51) for SUIT.

Task functional connectivity was analysed across the entire functional MRI run including rest and force blocks. The ANATICOR function in AFNI was incorporated to regress non-specific noise sources from the BOLD data including motion parameters, white matter, and CSF. The residual time series data (ANATICOR) for low visual feedback condition at each voxel was subtracted from its high visual feedback counterpart ($ANATICOR_\Delta$). After obtaining the residual time series, 3DTcorr1D function was used to compute Pearson's correlation coefficients between the time series of each region of interest and all other brain voxels, separately for each task. Seed regions of interest were placed within key nuclei of the cerebello-thalamo-basal ganglia-cortical circuit including the left and right dentate nucleus, ventral intermediate thalamic nucleus (VIM), globus pallidus internus (GPi), and sensorimotor cortex. The GPi and VIM are primary targets for deep brain stimulation (DBS) in dystonia and essential tremor, respectively (Koller *et al.*, 2001; Vidailhet *et al.*, 2005; Hung *et al.*, 2007; Papavassiliou *et al.*, 2008). The VIM has also emerged as a potential candidate for DBS in dystonic tremor (Morishita *et al.*, 2010; Hedera *et al.*, 2013; Cury *et al.*, 2017). Region of interest labelling of GPi and VIM were derived from the Basal Ganglia Human Area Template (Prodoehl *et al.*, 2008) and population-based stereotactic coordinates for VIM DBS (Papavassiliou *et al.*, 2008), respectively. For the cortex, we used a functional seed location derived from previous work (Archer *et al.*, 2018) in the sensorimotor cortex/inferior parietal lobule (SMC/IPL). We additionally used its mirror-symmetrical location to be consistent with left and right hemispheric placements of other seeds. Correlation coefficients were converted to z-scores using Fisher r-to-z transformations. High minus low functional connectivity (FC_Δ) maps were computed using independent-samples t-tests on the high minus low z-scores for each region of interest, while covarying for age and z-score related to that specific region of interest in the low visual feedback task. T-tests were limited to voxels activated in the task using a mask file generated by combining the within-group BOLD activation maps for the high visual feedback task across all three groups. The significance threshold was determined using 3dClustSim and set to $P < 0.005$ ($P < 0.05$ FWER-corrected) with a minimum cluster size of 675 mm^3 (ACF: 0.65, 4.71, 10.78). The larger cluster size for FC_Δ data compared to the $BOLD_\Delta$ was due to the inherent smoothness of the FC_Δ data.

We sought to determine whether functional connectivity was effective in classifying dystonic tremor and essential tremor groups. First, we generated a functional connectivity mask by combining the FC_Δ statistical maps for the dystonic versus essential tremor comparisons for all eight regions of interest (thresholded at $P < 0.05$ FWER-corrected). Next, we obtained the average z-scores from the $ANATICOR_\Delta$ time series for each dystonic tremor and essential tremor patient and across all voxels contained within the mask, separately for each region of interest. The average z-score for each patient and each region of interest was then entered into a binary logistic regression model with forward selection to determine the best set of independent variables that predicted group. Model accuracy was tested using ROC and LOOCV approaches.

Data availability

De-identified data are available from the corresponding author upon reasonable request.

Results

Change in force and tremor related to visual feedback

Within-group effects for mean force$_\Delta$ and RMSE$_\Delta$ were examined using one-sample t-tests. All groups had significantly positive mean force$_\Delta$ [$t(\geqslant 17) > 2.67$, $P < 0.02$] (Fig. 3A). All groups had significantly negative RMSE$_\Delta$ [$t(\geqslant 17) < -3.78$, $P < 0.002$], indicating error improved with visual feedback (Fig. 3B). One-way ANOVA models were not significant for mean force$_\Delta$ [$F(2,53) = 1.37$, $P = 0.2$] and RMSE$_\Delta$ [$F(2,53) = 1.59$, $P = 0.2$]. Within-group effects for force tremor$_\Delta$ were examined using one-sample Wilcoxon signed-rank tests. As expected, the control group did not demonstrate a significant force tremor$_\Delta$ score (W = 31, $P = 0.2$). In contrast, dystonic tremor (W = 166, $P < 0.002$) and essential tremor (W = 112, $P < 0.01$) groups demonstrated significantly positive force tremor$_\Delta$ scores, indicating increased tremor with increased visual feedback. A Kruskal-Wallis test on force tremor$_\Delta$ data yielded a significant main effect of group [$\chi^2(2) = 9.17$, $P = 0.01$]. Dunn's test revealed increased force tremor$_\Delta$ for dystonic tremor ($z = 2.35$, $P < 0.01$) and essential tremor ($z = 2.85$, $P < 0.01$) compared to controls, but dystonic tremor and essential tremor did not differ ($z = 0.57$, $P = 0.28$) (Fig. 3D).

Between-group effects of mean and standard deviation of peak force power and frequency were examined using Kruskal-Wallis tests and significant chi-squared values were decomposed using Dunn's test. Mean and standard deviation peak power did not differ between groups in the low, high, or high minus low feedback tasks [$\chi^2(2) > 6.1$, P-values > 0.051]. Group effects were uncovered for mean peak frequency in the low and high feedback tasks [$\chi^2(2) > 16.3$, P-values < 0.0005]. Essential tremor had higher mean peak frequency values compared to controls and dystonic tremor ($z > 13.13$, P-values < 0.05 FDR-corrected). A main effect was also uncovered for standard deviation peak frequency in the high
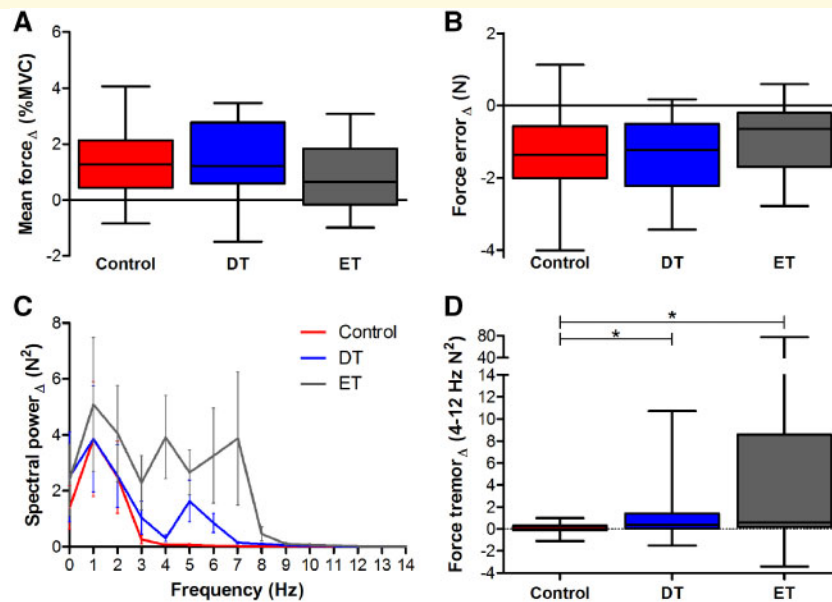
Figure 3 Statistical analyses for force variables. Box and whisker plot summaries for (**A**) mean force$_\Delta$, (**B**) force error$_\Delta$, (**C**) spectral power$_\Delta$ (0–14 Hz), and (**D**) force tremor$_\Delta$ (4–12 Hz) are shown for controls (red), dystonic tremor (DT, blue), and essential tremor (ET, grey). Asterisks represent a significant increase in force tremor$_\Delta$ for the dystonic tremor and essential tremor groups compared to controls ($P < 0.05$ FDR-corrected).

feedback task [$\chi^2(2) = 20.16$, $P = 0.00004$], where values were higher in essential tremor compared to controls and dystonic tremor ($z > 3.62$, P-values < 0.05 FDR-corrected) (Supplementary Fig. 1).

Between-group effects in BOLD$_\Delta$

BOLD$_\Delta$ amplitude for dystonic tremor was reduced relative to controls in frontal cortex, cingulate, and cerebellum (I–IV). Compared to controls, BOLD$_\Delta$ amplitude in essential tremor was reduced in sensory cortex, parietal cortex, middle frontal gyrus, middle temporal gyrus, inferior occipital gyrus, visual cortex, and cerebellum (I–IV, VI, VIIIb). BOLD$_\Delta$ in essential tremor was reduced relative to dystonic tremor in the sensorimotor cortex, inferior parietal lobule, cingulate, mesial premotor cortex, and visual cortex. In turn, BOLD$_\Delta$ in dystonic tremor was reduced compared to essential tremor in the middle frontal gyrus (Fig. 4 and Supplementary Table 1).
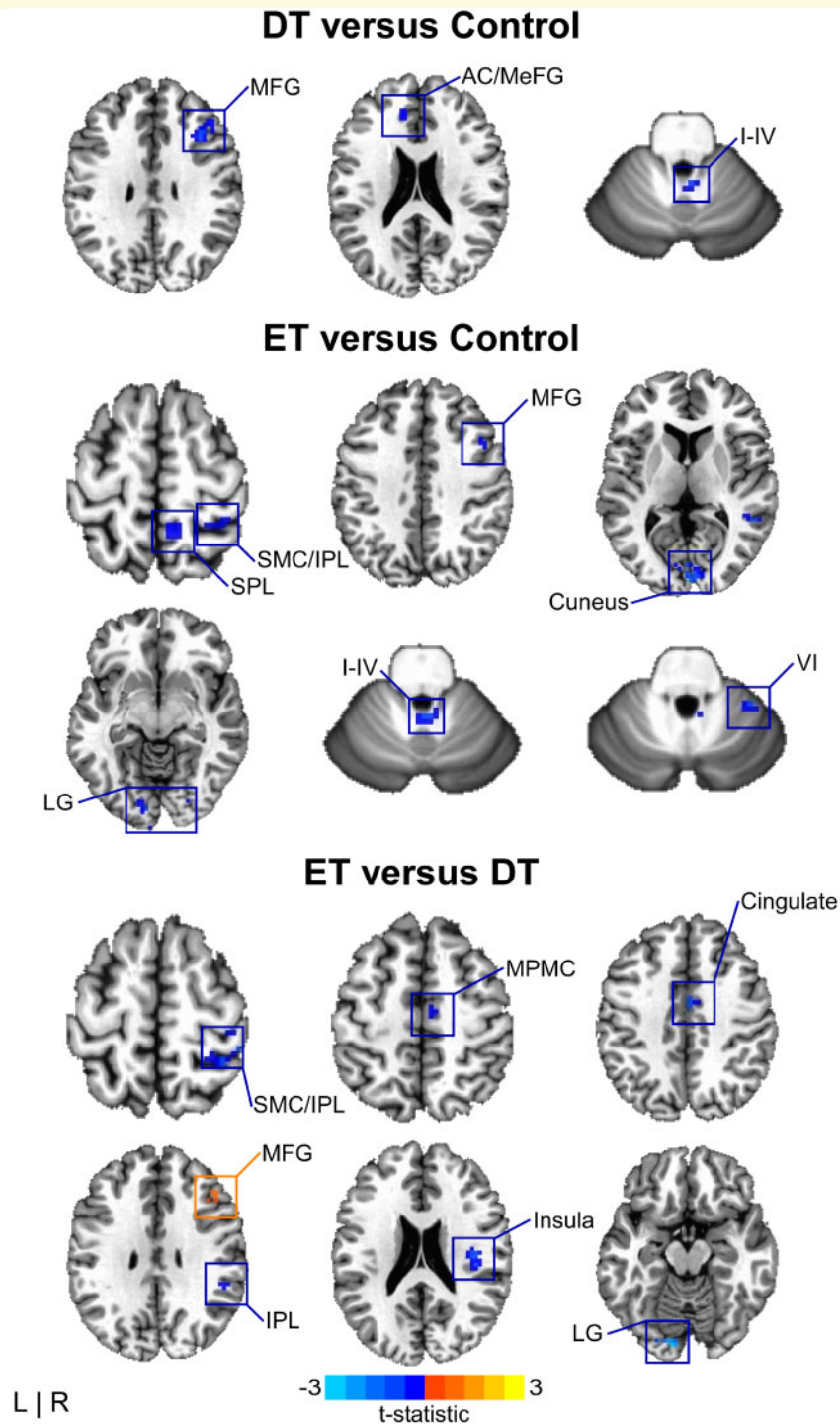
Between-group effects in FC$_\Delta$

Left and right SMC/IPL regions of interest revealed abnormal FC$_\Delta$ in dystonic tremor and essential tremor compared to controls within clusters comprising the sensorimotor cortex, premotor cortex, frontal cortex, parietal cortex, visual cortex, putamen and globus pallidus. The degree to which these areas were affected was greater in terms of cluster volume in dystonic tremor. Additionally, both SMC/IPL regions of interest in the dystonic tremor group showed reduced FC$_\Delta$ with multiple

cerebellar clusters (I–IV, V, VI, VIIb, VIIIa, VIIIb; crus I, vermis, and deep cerebellar nuclei), whereas cerebellar FC$_\Delta$ was not affected in essential tremor (Fig. 5 and Supplementary Table 2).

Dystonic tremor revealed extensive patterns of deficient FC$_\Delta$ for both SMC/IPL regions of interest compared to essential tremor (Fig. 6A). Left SMC/IPL FC$_\Delta$ was reduced in dystonic tremor within an ipsilateral cluster comprising the inferior parietal lobule; and bilateral clusters in sensorimotor cortex, premotor cortex, superior parietal lobule, temporal cortex, insula, visual cortex, middle occipital gyrus, cingulate, putamen, and cerebellum (VI, crus I and II, vermis). Right SMC/IPL FC$_\Delta$ was reduced in dystonic tremor within contralateral hemisphere clusters comprising parietal cortex, temporal cortex, and insula; ipsilateral clusters in sensorimotor cortex, premotor cortex, middle frontal gyrus, middle occipital gyrus, and middle temporal gyrus; and bilateral clusters comprising the cingulate, visual cortex, and cerebellum (I–IV, V, VI, VIIIa, vermis). Left SMC/IPL FC$_\Delta$ was reduced in essential tremor compared to dystonic tremor within contralateral clusters comprising the middle frontal gyrus and insula, whereas right SMC/IPL FC$_\Delta$ was reduced within contralateral clusters of the medial frontal gyrus and insula; and a bilateral cluster comprising paracentral lobule and cingulate.

Dystonic tremor and essential tremor revealed abnormal left and right GPi FC$_\Delta$ compared to controls within the premotor cortex, parietal cortex, and supplementary motor area. The degree to which these areas were affected was greater in terms of cluster volume in the dystonic

Figure 4 BOLD$_\Delta$ between-group effects. Spatial colour coded *t*-statistical maps representing the mean difference in BOLD$_\Delta$ amplitude for dystonic tremor (DT) versus controls (*top*), essential tremor (ET) versus controls (*middle*), and essential tremor versus dystonic tremor (*bottom*). Results are thresholded at *P* < 0.05 FWER-corrected. Positive (yellow-orange-red) values, denote a significantly positive difference for the contrast of interest, whereas negative (blue) values represent a significantly negative difference. I–IV, VI = cerebellar lobules I–IV and VI, respectively; AC = anterior cingulate; IPL = inferior parietal lobule; LG = lingual gyrus; MeFG = medial frontal gyrus; MFG = middle frontal gyrus; MPMC = mesial premotor cortex; SMC = sensorimotor cortex; SPL = superior parietal lobule.

tremor group. Dystonic tremor revealed additional abnormalities in FC$_\Delta$ compared to controls in sensorimotor cortex, frontal cortex, visual cortex, cingulate, insula, putamen, and thalamus, and extensively throughout the cerebellum (I–IV, VI, V, VIIb, VIIIa, VIIIb, IX, vermis) (Fig. 5 and Supplementary Table 3).
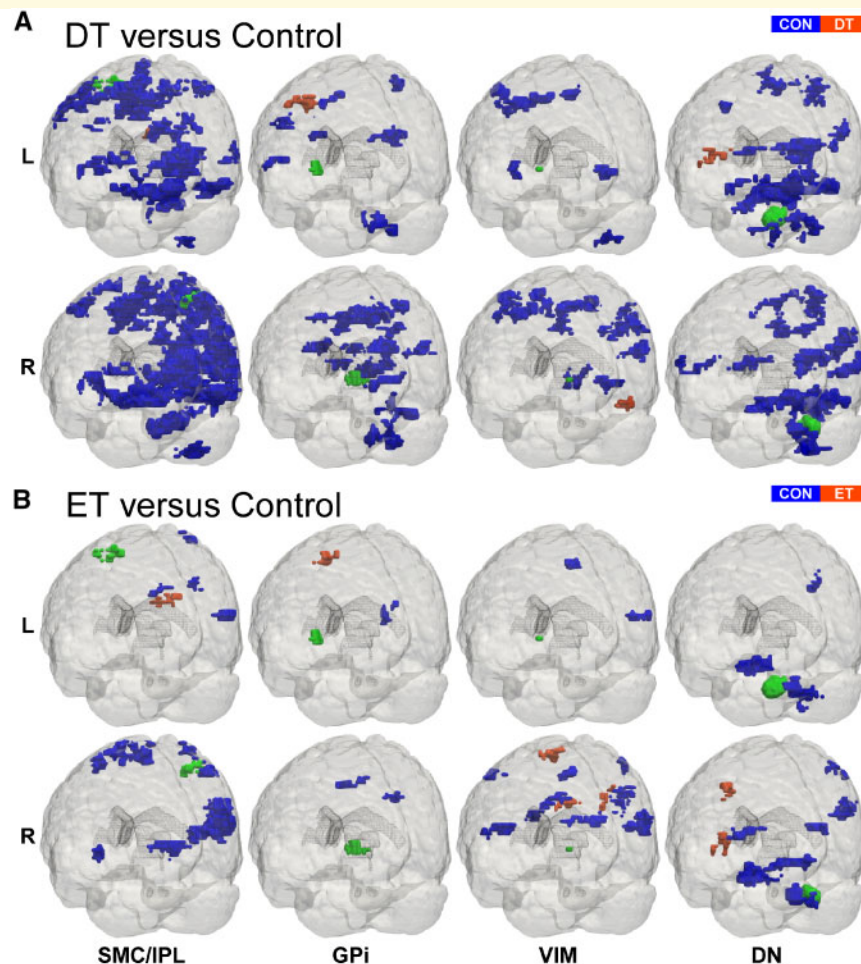
Figure 5 Patient versus control FC$_\Delta$ effects. 3D rendering (Madan, 2015) of whole-brain *t*-statistical maps comparing FC$_\Delta$ for (**A**) dystonic tremor (DT) versus controls (CON) and (**B**) essential tremor (ET) versus controls (*bottom*). The *x*-axis denotes the seed region of interest in the SMC/IPL, GPi, VIM, and dentate nucleus (DN). The *y*-axis in each panel denotes the location of the seed region of interest in the left (L) and the right (R) hemispheres. In each panel, positive (red-orange) clusters, denote significantly increased FC$_\Delta$ with the seed region of interest in the patient group (i.e. dystonic tremor or essential tremor) relative to controls, whereas negative (blue) clusters, denote significantly reduced FC$_\Delta$ with the seed region of interest in patient groups relative to controls ($P < 0.05$ FWER-corrected).

GPi FC$_\Delta$ for both regions of interest was impaired in dystonic tremor compared to essential tremor (Fig. 6B). Left GPi FC$_\Delta$ was reduced in dystonic tremor within contralateral clusters in sensorimotor cortex, superior parietal lobule, and fusiform gyrus; and bilateral clusters comprising paracentral lobule and inferior parietal lobule. Right GPi FC$_\Delta$ was reduced in dystonic tremor within ipsilateral clusters of sensorimotor cortex, inferior parietal lobule, insula, and putamen; and bilateral paracentral lobule and cingulate.

VIM seeds in the dystonic tremor group revealed FC$_\Delta$ abnormalities compared to controls in sensorimotor cortex, frontal cortex, parietal cortex, cingulate, precuneus, visual cortex, putamen, globus pallidus, and cerebellum (VIIIa, VIIIb, VIIb). VIM FC$_\Delta$ in the essential tremor group was reduced compared to controls in the sensorimotor cortex, frontal cortex, parietal cortex, temporal cortex, and cingulate (Fig. 5 and Supplementary Table 4).

Left VIM FC$_\Delta$ was reduced in dystonic tremor compared to essential tremor within bilateral clusters in the cuneus and insula; ipsilateral clusters in the sensorimotor cortex, inferior parietal lobule, and putamen; and contralateral clusters in the medial frontal gyrus, visual cortex, superior temporal gyrus, and cerebellum (V, VI, crus I). Left VIM FC$_\Delta$ was reduced in essential tremor compared to dystonic tremor in a single contralateral cluster comprising the temporal cortex. Right VIM FC$_\Delta$ was reduced in dystonic tremor compared to essential tremor in bilateral clusters in sensorimotor cortex and medial frontal gyrus; ipsilateral visual cortex, putamen, superior temporal gyrus, and insula; and contralateral inferior parietal lobule (Fig. 7A).

Left and right dentate nucleus regions of interest in dystonic tremor and essential tremor revealed abnormal FC$_\Delta$ compared to controls within clusters of the sensorimotor cortex, premotor cortex, frontal cortex, parietal cortex,
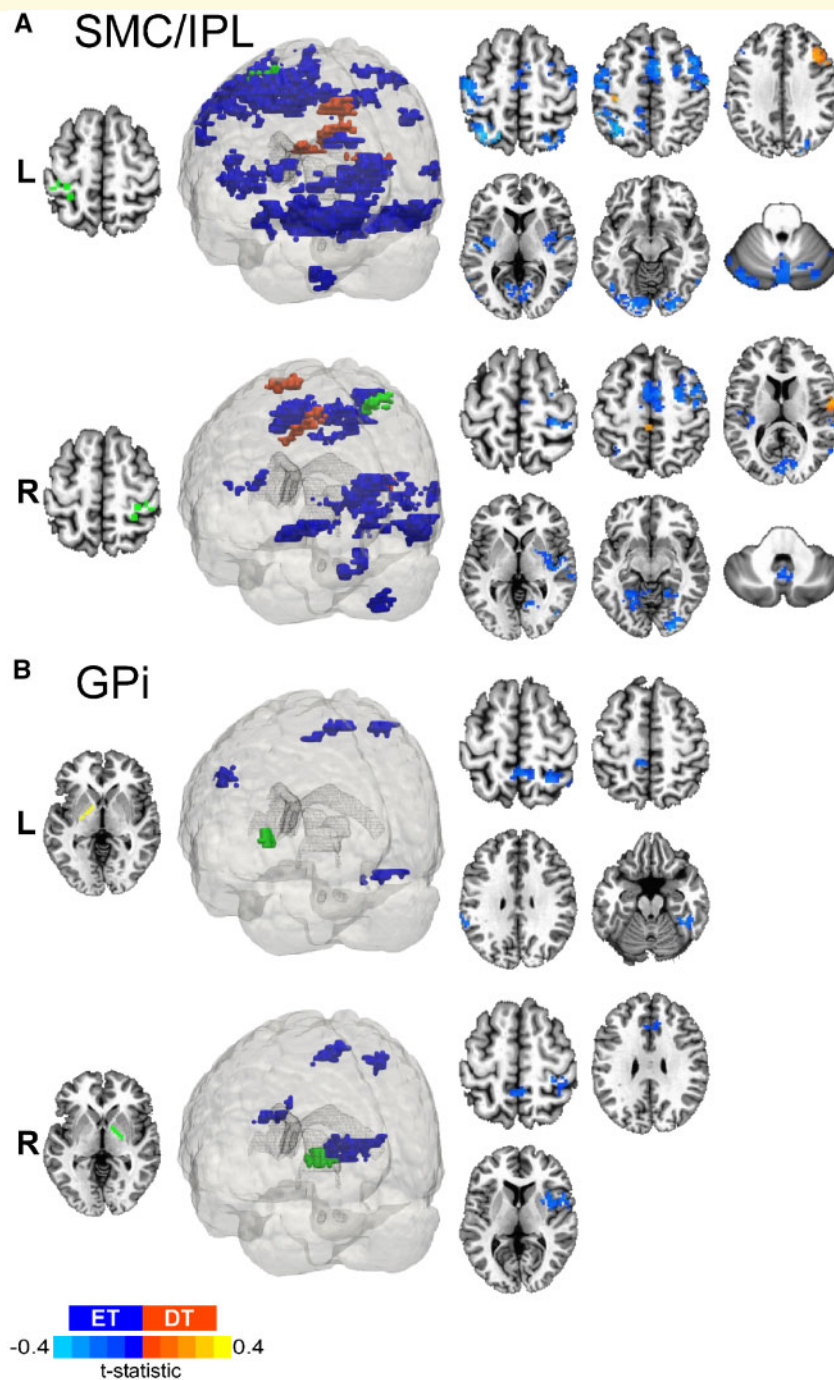
Figure 6 Dystonic tremor versus essential tremor SMC/IPL and GPi FC$_\Delta$. 3D rendering and axial slice representation of whole-brain *t*-statistical maps comparing FC$_\Delta$ of (**A**) SMC/IPL and (**B**) GPi for the dystonic tremor (DT) versus essential tremor (ET) comparison. Seed regions of interest are shown in green and the *top* and *bottom* panels depict the between-group FC$_\Delta$ effects originating from the left (L) and right (R) seeds, respectively. In each panel, positive (red-orange) clusters denote significantly increased FC$_\Delta$ with the seed region of interest in the dystonic tremor group compared to essential tremor group, whereas negative (blue) clusters denote significantly reduced FC$_\Delta$ with the seed region of interest in the dystonic tremor group compared to essential tremor group (*P* < 0.05 FWER-corrected).

visual cortex, temporal cortex, insula, and cerebellum (I–IV, V, VI, crus II, vermis). The degree to which these regions were affected was greater in terms of cluster volume in the dystonic tremor group. Moreover, the dystonic tremor group revealed additional FC$_\Delta$ impairments relative

to controls in the cerebellum (VIIb, VIIIa, VIIIb, crus I) (Fig. 5 and Supplementary Table 5).

Left dentate nucleus FC$_\Delta$ was reduced in dystonic tremor compared to essential tremor within ipsilateral inferior parietal lobule, occipital cortex, and cerebellum (VI); and

bilateral clusters in sensorimotor cortex, mesial premotor cortex, frontal cortex, superior parietal lobule, paracentral lobule, and visual cortex. Right dentate nucleus FC_Δ was reduced in dystonic tremor compared to essential tremor within the ipsilateral sensorimotor cortex, middle frontal gyrus, superior parietal lobule, paracentral lobule, visual cortex, temporal cortex, and cerebellum (V, VI, vermis); and a bilateral cluster in frontal cortex. Left dentate nucleus FC_Δ was reduced in essential tremor compared to dystonic tremor in a single ipsilateral cluster in inferior parietal lobule, whereas right dentate nucleus FC_Δ was reduced in essential tremor in inferior parietal lobule bilaterally (Fig. 7B).

Patient group classification

Spectral power$_\Delta$ data for the 0–3 and 4–12 Hz ranges (shown in Fig. 3C) combined with standard deviation of peak force frequency$_\Delta$ yielded moderately effective group classification in the ROC analysis (AUC = 0.77; 83% sensitivity, 65% specificity) and the LOOCV analysis [mean squared error (MSE) = 0.4]. The combined functional connectivity z-scores across all eight regions of interest in the high minus low feedback task provided an advantage in classifying patient groups compared to clinical tremor data alone (ROC: AUC = 0.89; 78% sensitivity, 90% specificity; LOOCV: MSE = 0.29). ROC classification was also evident when combining force (0–3 and 4–12 Hz spectral power$_\Delta$ and standard deviation peak force frequency$_\Delta$) and FC_Δ z-scores (ROC: AUC = 0.94; 78% sensitivity, 100% specificity; LOOCV: MSE = 0.34). The results of the logistic regression determined that left SMC/IPL FC_Δ ($F = 8.46$, $P = 0.004$) and standard deviation peak force frequency$_\Delta$ ($F = 4.83$, $P = 0.028$) were significant predictors of patient cohort for connectivity and force data, respectively. Forward selection determined that left SMC/IPL FC_Δ z-scores best predicted patient cohort ($F = 8.46$, $P = 0.004$). Left SMC/IPL FC_Δ z-scores yielded an LOOCV MSE value of 0.19, suggesting high patient group classification accuracy (Supplementary Table 6).

Effect of head motion of FC_Δ

To test whether cervical dystonia and dystonic head tremor in dystonic tremor contributed to MRI signal distortion artefacts and loss of connectivity strength, we first obtained the average motion (mm) for censored repetition times across low and high visual feedback tasks for each participant and submitted values to a one-way ANOVA with Welch correction. Average head motion across control (0.12 ± 0.03 mm), dystonic tremor (0.18 ± 0.09 mm), and essential tremor (0.14 ± 0.05 mm) groups revealed a significant main effect [$F(2,30) = 4.76$, $P < 0.02$]. Independent-samples *t*-tests revealed increased motion in dystonic tremor compared to controls [$t(22) = 2.94$, $P < 0.02$] but not essential tremor [$t(28) = 1.95$, $P = 0.18$]. Further examination of the data revealed that this effect was driven by two dystonic tremor patients in particular with head

motion averages at 0.38 and 0.35 mm, and the average of the remaining subjects was 0.16 mm. Removal of these two subjects from the one-way ANOVA model failed to yield a significant main effect for motion. Next, we examined the between-group FC_Δ effects for the dystonic tremor-essential tremor comparisons in all regions of interest with and without the inclusion of the two dystonic tremor patients. Results showed that FC_Δ effects for all regions of interest did not differ when outlier motion dystonic tremor patients were excluded from the analysis (Supplementary Fig. 2). Finally, to determine if motion was related to FC_Δ, we performed Pearson's correlations between average head motion across low and high visual feedback tasks and average z-scores from the connectivity analysis. This analysis revealed non-significant correlations between motion and z-scores for any of the regions of interest in the dystonic tremor, essential tremor, and control groups ($R^2 < 0.15$, *P*-values > 0.05), further indicating that head motion is not driving these results.

Discussion

This study examined the effects of visual feedback on force tremor and associated changes in BOLD activation and connectivity during the completion of a grip-force task in dystonic tremor patients. The findings here are convincing that like dystonia, dystonic tremor is a network disorder involving large-scale BOLD amplitude and connectivity changes across cortical, basal ganglia, and cerebellar regions. A secondary goal of the current study was to develop a perspective for network-level BOLD activation and connectivity that distinguishes dystonic tremor from essential tremor, which yielded several important findings. Increased visual feedback exacerbated force tremor during the grip-force task in both patient groups. Dystonic tremor and essential tremor were characterized by distinct BOLD$_\Delta$ amplitude abnormalities in higher-level cortical and visual regions but not in the cerebellum. Furthermore, dystonic tremor was characterized by widespread reductions in FC_Δ compared to essential tremor including cortical, visual, basal ganglia, and cerebellar regions, whereas essential tremor demonstrated only minor cortical FC_Δ reductions compared to dystonic tremor. Importantly, FC_Δ z-scores were able to separate dystonic tremor and essential tremor patient cohorts with very good sensitivity and specificity. These findings provide support that dystonic tremor involves distinct brain networks from essential tremor, and points to large-scale network connectivity as a key feature distinguishing these disorders.

Visual feedback increases force tremor in dystonic tremor

Increasing visual feedback produced positive mean force tremor$_\Delta$ in dystonic tremor and essential tremor compared to controls. Exacerbated tremor within the 4–12 Hz power spectral range replicates our prior work in essential tremor
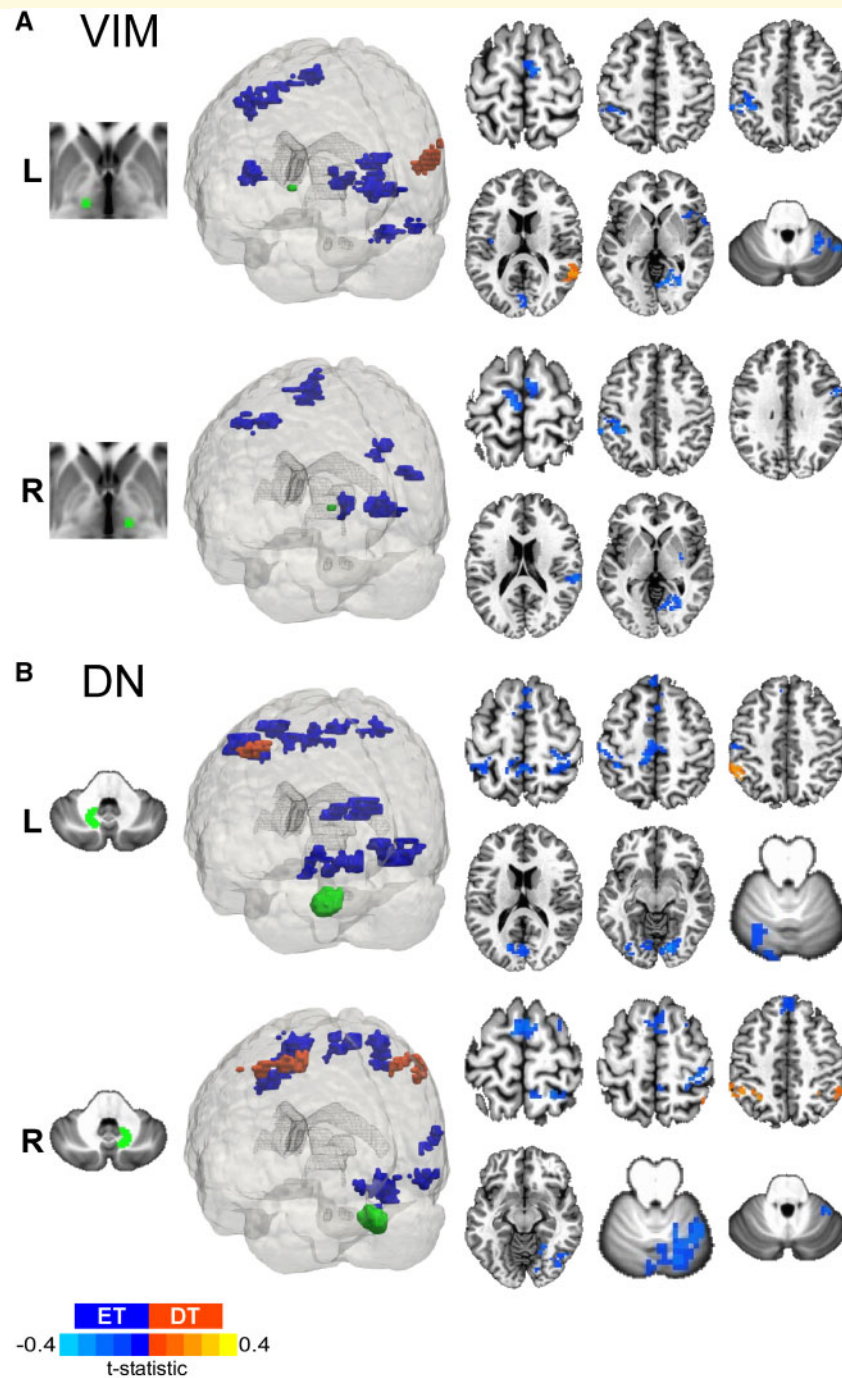
Figure 7 Dystonic tremor versus essential tremor VIM and dentate nucleus FC$_\Delta$. 3D rendering and axial slice representation of whole-brain *t*-statistical maps comparing FC$_\Delta$ of (**A**) VIM thalamus and (**B**) dentate nucleus (DN) for the dystonic tremor (DT) versus essential tremor (ET) comparison. Seed regions of interest are shown in green and the *top* and *bottom* panels depict the between-group FC$_\Delta$ effects originating from the left (L) and right (R) seeds, respectively. In each panel, positive (red-orange) clusters denote significantly increased FC$_\Delta$ with the seed region of interest in the dystonic tremor group compared to essential tremor group, whereas negative (blue) clusters denote significantly reduced FC$_\Delta$ with the seed region of interest in the dystonic tremor group compared to essential tremor group ($P < 0.05$ FWER-corrected).

(Archer *et al.*, 2018) and supports the hypothesis that increasing the availability of visual information worsens tremor (Feys *et al.*, 2003; Keogh *et al.*, 2004; Gironell *et al.*, 2012). Previous studies have classified dystonic tremor and essential tremor based on physiological mechanisms of tremor (Münchau *et al.*, 2001; Shaikh *et al.*, 2008). Some studies, which have used accelerometer recordings and filter the low frequency rhythm, have reported tremor that is more irregular in dystonic tremor compared to essential tremor (Shaikh *et al.*, 2008; Bove

et al., 2018). This was not apparent in the current study, as essential tremor had increased standard deviation of peak force frequency compared to controls and dystonic tremor. We believe this is likely related to the isometric force task. In isometric force for healthy adults and those with Parkinson's disease, peak power is around 1 Hz with residual tremor power between 4–8 Hz (Vaillancourt *et al.*, 2001). The same can be seen for healthy older and young adults (Vaillancourt *et al.*, 2003). If a patient has considerable tremor, then the power in the 4–8 Hz band increases to be greater than the power in the 0–2 Hz band. Thus, in essential tremor patients who have more tremor than the dystonic tremor patients at the hand producing force, the peak frequency may occur at either low or tremor frequencies thereby increasing variability.

Distinct cortical and visual BOLD difference impairments in dystonic tremor and essential tremor

$BOLD_\Delta$ amplitude in dystonic tremor was reduced in the frontal cortex and cerebellum (I–IV) compared to controls. Notably, $BOLD_\Delta$ amplitude in the primary visual cortex was not affected. Although our behavioural results reinforce the assertion that tremor severity is influenced by availability of visual information (Feys *et al.*, 2003; Keogh *et al.*, 2004; Gironell *et al.*, 2012), the $BOLD_\Delta$ results suggest visual feedback-induced tremor exacerbation in dystonic tremor need not be coupled to associated dysfunction of visual regions akin to present and prior evidence in essential tremor (Neely *et al.*, 2015; Archer *et al.*, 2018). Functional abnormalities of prefrontal and cerebellar regions in patients with cervical dystonia have been previously reported, although it was unclear whether these patients also had tremor (Galardi *et al.*, 1996; Burciu *et al.*, 2017; Filip *et al.*, 2017). Similar to our findings, Kirke *et al.* (2017) reported deficient activation of the middle frontal gyrus and cerebellum (lobule VII) in SD/DT_V relative to spasmodic dysphonia. Discrepant cerebellar abnormalities in our study (lobule I–IV) compared to their work may be attributable to task modality or phenotypic differences across the two cohorts. Our study shows impaired adaptation of BOLD signal in response to visual feedback similar to essential tremor, and further implicates the role of cerebello-frontal cortex network in the pathogenesis of dystonic tremor.

Dystonic tremor and essential tremor groups demonstrated functionally distinct higher-level cortical abnormalities. $BOLD_\Delta$ amplitude of the middle frontal gyrus was reduced in dystonic tremor relative to both control and essential tremor groups. In turn, activation of the sensorimotor cortex and inferior parietal lobule were reduced in essential tremor relative to both control and dystonic tremor groups. Dysfunction of the parieto-motor network in essential tremor has been interpreted to possibly reflect a cortical domain of increased kinetic tremor oscillations. For example, increased force $tremor_\Delta$ in essential tremor was found to correlate with sensorimotor and parietal $BOLD_\Delta$ signal (Archer *et al.*, 2018). Moreover, high-density EEG in essential tremor patients revealed reduced sensorimotor beta-band desynchronization and bi-directional connectivity between the motor and parietal cortices that was related to feedback induced exacerbation of force tremor of the arm (Roy *et al.*, 2018). These differences in findings for dystonic tremor and essential tremor suggest functionally disparate higher-level cortical mechanisms that will need further exploration.

Functional abnormalities of the cerebellum have been a consistent finding in cervical dystonia (Magyar-Lehmann *et al.*, 1997; Burciu *et al.*, 2017; Filip *et al.*, 2017) and essential tremor (Bucher *et al.*, 1997; Buijink *et al.*, 2015*a*, *b*; Neely *et al.*, 2015; Broersma *et al.*, 2016; Archer *et al.*, 2018). Similar to these studies, we uncovered reduced cerebellar $BOLD_\Delta$ amplitude in dystonic tremor (lobule I–IV) and essential tremor (lobules I–IV, VI, and VIIIb) compared to controls, although no difference between patient groups was uncovered. Kirke *et al.* (2017) recently interpreted common and uncommon functional substrates between patients with spasmodic dysphonia and SD/DT_V to reflect that dystonia and dystonic tremor represent heterogeneous disorders, and that dystonic tremor is likely positioned between dystonia and essential tremor based on symptomology and brain abnormalities common to both dystonia and essential tremor. Our $BOLD_\Delta$ findings may further support this interpretation given that dystonic tremor and essential tremor revealed common cerebellar and distinct higher-level (i.e. sensorimotor cortex, inferior parietal lobule, visual cortex, middle frontal gyrus) neural signatures.

Distinct network-level functional connectivity changes in dystonic tremor and essential tremor

The notion that a distributed motor network is involved in the pathogeneses of dystonia and essential tremor incites motivation to examine network-level connectivity dynamics among cortical, basal ganglia, and cerebellar systems. Relative to controls and independent of the region of interest, increased visual feedback in dystonic tremor caused changes in inter- and intra-regional FC_Δ interactions among a widely distributed network within and beyond the cerebello-basal ganglia-cortical pathway. SMC/IPL and dentate nucleus seeds revealed bi-directional cortico-cerebellar changes in FC_Δ. The SMC/IPL also showed abnormal FC_Δ with basal ganglia regions and the GPi showed abnormal FC_Δ with cortical and cerebellar regions. Interestingly, whereas $BOLD_\Delta$ amplitude of visual regions was not affected in dystonic tremor, all regions of interest revealed abnormal FC_Δ with visual cortex, suggesting that visual feedback-induced tremor exacerbation in dystonic tremor may relate to dysfunctional connectivity and not

activation. Functional connectivity in cervical dystonia has received little attention and to our knowledge has not been examined in dystonic tremor. Delnooz *et al.* (2013) reported abnormal resting state connectivity of sensorimotor, visual, and executive control (prefrontal, cingulate, parietal) networks. Li *et al.* (2017) recently reported higher connectivity in cervical dystonia in the cortex, basal ganglia, thalamus, and cerebellum originating from a bilateral region of interest in the precentral gyrus implicated in isometric head movement. Here, we show that cortical (prefrontal, premotor, parietal, temporal, visual), basal ganglia, and cerebellar FC_Δ originating from a sensorimotor seed location is abnormal in dystonic tremor and the majority of clusters showed reduced FC_Δ. The extent of FC_Δ abnormalities in dystonic tremor may be primary to dystonia itself, but we cannot confirm this in the current study. That is, changes in FC_Δ of the cortex, basal ganglia, thalamus, and cerebellum support the notion that cervical dystonia is a disorder affecting widely distributed functional brain networks (Neychev *et al.*, 2011; Prudente *et al.*, 2014; Jinnah *et al.*, 2017). Future studies including a subset of dystonia patients without tremor is important to better understanding the pathophysiological distinction between dystonia and dystonic tremor, and how these functional substrates relate to essential tremor.

The essential tremor group revealed abnormal FC_Δ relative to controls independent of the region of interest. The magnitude of the effects for each region of interest in terms of number of regional dysfunctional connections and cluster volume were typically less than that of the dystonic tremor versus control comparison. Future work involving weighted graph theory network analysis (Rubinov and Sporns, 2010) would be useful in determining whether the strength of functional connections is effective in distinguishing dystonic tremor and essential tremor. FC_Δ between the SMC/IPL and sensorimotor, premotor, prefrontal, parietal, temporal, visual and basal ganglia regions was abnormal in essential tremor relative to controls. This finding is important because the sensorimotor cortex and inferior parietal lobule have been consistently shown to be hypoactive in essential tremor here and in prior work (Archer *et al.*, 2018). Evidence that the cortico-cortico connectivity originating from this region is abnormal in essential tremor is in line with previous studies (Fang *et al.*, 2013; Gallea *et al.*, 2015). A recent study in essential tremor revealed changes in resting state functional connectivity within the VIM-motor cortex-cerebellar circuit (Fang *et al.*, 2016). Here, essential tremor revealed abnormal FC_Δ of the VIM thalamus within a distributed cortical network but not the cerebellum. Essential tremor demonstrated abnormal FC_Δ originating from the dentate nucleus to cortical regions, but not originating from the SMC/IPL to cerebellar regions. Abnormal cerebello-cortico FC_Δ fits well with prior evidence that functional coupling between the cerebellum and sensorimotor cortex is disturbed in essential tremor during the completion of a motor task (Buijink *et al.*, 2015b; Neely *et al.*, 2015). Distinct FC_Δ

abnormalities were revealed in the patient group comparisons. It was clear that FC_Δ was impaired to a greater degree in dystonic tremor independent of the seed region. For seed locations in the SMC/IPL, VIM thalamus, and dentate nucleus, FC_Δ for dystonic tremor was reduced compared to essential tremor across a widely distributed network involving cortical, subcortical, and cerebellar regions, whereas reductions in cortical FC_Δ primarily characterized essential tremor relative to dystonic tremor. As well, GPi FC_Δ was reduced in dystonic tremor compared to essential tremor across multiple cortical and basal ganglia regions. Most importantly, combining FC_Δ z-scores across all regions of interest yielded effective classification of patient groups in the ROC analysis (AUC = 0.89; 78% sensitivity, 90% specificity) and LOOCV analysis (MSE = 0.29). Collectively, these findings support distinct network-level connectivity within and beyond the cerebello-basal ganglia-cortical network despite similar feedback-dependent task performance and tremor outcomes.

Conclusions

The current study provides novel evidence of distinct task-related $BOLD_\Delta$ amplitude and FC_Δ changes in dystonic tremor and essential tremor. Dystonic tremor and essential tremor are characterized by distinct functional activation signatures in higher-level cortical and visual regions, but common cerebellar impairments. A salient finding was that the magnitude of the FC_Δ effects was more widespread in the dystonic tremor group, affecting cortical, subcortical, and cerebellar systems independent of the region of interest. Furthermore, these differences in FC_Δ across cortical, subcortical, and cerebellar regions proved effective in classifying dystonic tremor and essential tremor groups with very good sensitivity and specificity. This study provides a fresh perspective that network-level activation and connectivity differ substantially between dystonic tremor and essential tremor and should be further explored in future studies for improved diagnostic and therapeutic strategies.

Acknowledgements

Funding

Competing interests

Supplementary material

Supplementary material is available at *Brain* online.

References

Albanese A, Bhatia K, Bressman SB, Delong MR, Fahn S, Fung VS, et al. Phenomenology and classification of dystonia: a consensus update. Mov Disord 2013; 28: 863–73.

Archer DB, Coombes SA, Chu WT, Chung JW, Burciu RG, Okun MS, et al. A widespread visually-sensitive functional network relates to symptoms in essential tremor. Brain 2018; 141: 472–85.

Argyelan M, Carbon M, Niethammer M, Uluğ AM, Voss HU, Bressman SB, et al. Cerebellothalamocortical connectivity regulates penetrance in dystonia. J Neurosci 2009; 29: 9740–7.

Battistella G, Fuertinger S, Fleysher L, Ozelius LJ, Simonyan K. Cortical sensorimotor alterations classify clinical phenotype and putative genotype of spasmodic dysphonia. Eur J Neurol 2016; 23: 1517–27.

Battistella G, Termsarasab P, Ramdhani RA, Fuertinger S, Simonyan K. Isolated focal dystonia as a disorder of large-scale functional networks. Cereb Cortex 2017; 27: 1203–15.

Benjamini Y, Hochberg Y. Controlling the false discovery rate: a practical and powerful approach to multiple testing. J R Stat Soc Ser B Stat Methodol 1995; 57: 289–300.

Bhatia KP, Bain P, Bajaj N, Elble RJ, Hallett M, Louis ED, et al. Consensus Statement on the classification of tremors. from the task force on tremor of the International Parkinson and Movement Disorder Society. Mov Disord 2018; 33: 75–87.

Bove F, Di Lazzaro G, Mulas D, Cocciolillo F, Di Giuda D, Bentivoglio AR. A role for accelerometry in the differential diagnosis of tremor syndromes. Funct Neurol 2018; 33: 45–9.

Britton TC, Thompson PD, Day BL, Rothwell JC, Findley LJ, Marsden CD. Rapid wrist movements in patients with essential tremor. The critical role of the second agonist burst. Brain 1994; 117 (Pt 1): 39–47.

Broersma M, van der Stouwe AMM, Buijink AWG, de Jong BM, Groot PFC, Speelman JD, et al. Bilateral cerebellar activation in unilaterally challenged essential tremor. Neuroimage Clin 2016; 11: 1–9.

Bucher SF, Seelos KC, Dodel RC, Reiser M, Oertel WH. Activation mapping in essential tremor with functional magnetic resonance imaging. Ann Neurol 1997; 41: 32–40.

Buijink AW, Broersma M, van der Stouwe AM, van Wingen GA, Groot PF, Speelman JD, et al. Rhythmic finger tapping reveals cerebellar dysfunction in essential tremor. Parkinsonism Relat Disord 2015a; 21: 383–8.

Buijink AW, van der Stouwe AM, Broersma M, Sharifi S, Groot PF, Speelman JD, et al. Motor network disruption in essential tremor: a functional and effective connectivity study. Brain 2015b; 138: 2934–47.

Burciu RG, Hess CW, Coombes SA, Ofori E, Shukla P, Chung JW, et al. Functional activity of the sensorimotor cortex and cerebellum relates to cervical dystonia symptoms. Hum Brain Mapp 2017; 38: 4563–73.

Coombes SA, Corcos DM, Sprute L, Vaillancourt DE. Selective regions of the visuomotor system are related to gain-induced changes in force error. J Neurophysiol 2010; 103: 2114–23.

Cury, RG, Fraix V, Castrioto A, Pérez Fernández MA, Krack P, Chabardes S, et al. Thalamic deep brain stimulation for tremor in Parkinson disease, essential tremor, and dystonia. Neurology 2017; 89: 1416–23.

Defazio G, Conte A, Gigante AF, Fabbrini G, Berardelli A. Is tremor in dystonia a phenotypic feature of dystonia? Neurology 2015; 84: 1053–9.

Defazio G, Gigante AF, Abbruzzese G, Bentivoglio AR, Colosimo C, Esposito M, et al. Tremor in primary adult-onset dystonia: prevalence and associated clinical features. J Neurol Neurosurg Psychiatry 2013; 84: 404–8.

Delnooz CC, Pasman JW, Beckmann CF, van de Warrenburg BP. Task-free functional MRI in cervical dystonia reveals multi-network changes that partially normalize with botulinum toxin. PLoS One 2013; 8: e62877.

Delnooz CC, Pasman JW, Beckmann CF, van de Warrenburg BP. Altered striatal and pallidal connectivity in cervical dystonia. Brain Struct Funct 2015; 220: 513–23.

Deuschl G, Bain P, Brin M. Consensus statement of the Movement Disorder Society on tremor. Ad Hoc Scientific Committee. Mov Disord 1998; 13 (Suppl 3): 2–23.

Deuschl G, Elble RJ. The pathophysiology of essential tremor. Neurology 2000; 54: S14–20.

Deuschl G, Heinen F, Guschlbauer B, Schneider S, Glocker FX, Lücking CH. Hand tremor in patients with spasmodic torticollis. Mov Disord 1997; 12: 547–52.

Diedrichsen J. A spatially unbiased atlas template of the human cerebellum. Neuroimage 2006; 33: 127–38.

Diedrichsen J, Balsters JH, Flavell J, Cussans E, Ramnani N. A probabilistic MR atlas of the human cerebellum. Neuroimage 2009; 46: 39–46.

Elble RJ. Physiologic and essential tremor. Neurology 1986; 36: 225–31.

Elble RJ, Higgins C, Leffler K, Hughes L. Factors influencing the amplitude and frequency of essential tremor. Mov Disord 1994; 9: 589–96.

Erro R, Rubio-Agusti I, Saifee TA, Cordivari C, Ganos C, Batla A, et al. Rest and other types of tremor in adult-onset primary dystonia. J Neurol Neurosurg Psychiatry 2014; 85: 965–8.

Fang W, Chen H, Wang H, Zhang H, Puneet M, Liu M, et al. Essential tremor is associated with disruption of functional connectivity in the ventral intermediate nucleus–motor cortex–cerebellum circuit. Hum Brain Mapp 2016; 37: 165–78.

Fang W, Lv F, Luo T, Cheng O, Liao W, Sheng K, et al. Abnormal regional homogeneity in patients with essential tremor revealed by resting-state functional MRI. PLoS One 2013; 8: e69199.

Feys P, Helsen WF, Liu X, Lavrysen A, Loontjens V, Nuttin B, et al. Effect of visual information on step-tracking movements in patients with intention tremor due to multiple sclerosis. Mult Scler 2003; 9: 492–502.

Filip P, Gallea C, Lehéricy S, Bertasi E, Popa T, Mareček R, et al. Disruption in cerebellar and basal ganglia networks during a visuospatial task in cervical dystonia. Mov Disord 2017; 32: 757–68.

Galardi G, Perani D, Grassi F, Bressi S, Amadio S, Antoni M, et al. Basal ganglia and thalamo-cortical hypermetabolism in patients with spasmodic torticollis. Acta Neurol Scand 1996; 94: 172–6.

Gallea C, Popa T, García-Lorenzo D, Valabregue R, Legrand AP, Marais L, et al. Intrinsic signature of essential tremor in the cerebello-frontal network. Brain 2015; 138: 2920–33.

Gironell A, Ribosa-Nogué R, Pagonabarraga J. Withdrawal of visual feedback in essential tremor. Parkinsonism Relat Disord 2012; 18: 402–3.

Hedera P, Phibbs FT, Dolhun R, Charles PD, Konrad PE, Niemat JS, et al. Surgical targets for dystonic tremor: considerations between the globus pallidus and ventral intermediate thalamic nucleus. Parkinsonism Relat Disord 2013; 19: 684–6.

Hung SW, Hamani C, Lozano AM, Poon YY, Piboolnurak P, Miyasaki JM, et al. Long-term outcome of bilateral pallidal deep brain stimulation for primary cervical dystonia. Neurology 2007; 68: 457–9.

Jinnah HA, Neychev V, Hess EJ. The anatomical basis for dystonia: the motor network model [Review]. Tremor Other Hyperkinet Mov (N Y) 2017; 7: 506.

Keogh J, Morrison S, Barrett R. Augmented visual feedback increases finger tremor during postural pointing. Exp Brain Res 2004; 159: 467–77.

Kirke DN, Battistella G, Kumar V, Rubien-Thomas E, Choy M, Rumbach A, et al. Neural correlates of dystonic tremor: a multimodal study of voice tremor in spasmodic dysphonia. Brain Imaging Behav 2017; 11: 166–75.

Koller WC, Lyons KE, Wilkinson SB, Troster AI, Pahwa R. Long-term safety and efficacy of unilateral deep brain stimulation of the thalamus in essential tremor. Mov Disord 2001; 16: 464–8.

Li Z, Prudente CN, Stilla R, Sathian K, Jinnah HA, Hu X. Alterations of resting-state fMRI measures in individuals with cervical dystonia. Hum Brain Mapp 2017; 38: 4098–108.

Madan CR. Creating 3D visualizations of MRI data: A brief guide. F1000Res 2015; 4: 466.

Magyar-Lehmann S, Antonini A, Roelcke U, Maguire RP, Missimer J, Meyer M, et al. Cerebral glucose metabolism in patients with spasmodic torticollis. Mov Disord 1997; 12: 704–8.

Morishita T, Foote KD, Haq IU, Zeilman P, Jacobson, Okun MS. Should we consider Vim thalamic deep brain stimulation for select cases of refractory dystonic tremor. Stereotact Funct Neurosurg 2010; 88: 98–104.

Münchau A, Schrag A, Chuang C, MacKinnon CD, Bhatia KP, Quinn NP, et al. Arm tremor in cervical dystonia differs from essential tremor and can be classified by onset age and spread of symptoms. Brain 2001; 124: 1765–76.

Neely KA, Kurani AS, Shukla P, Planetta PJ, Wagle Shukla A, Goldman JG, et al. Functional brain activity relates to 0–3 and 3–8 Hz force oscillations in essential tremor. Cereb Cortex 2015; 25: 4191–202.

Neychev VK, Gross RE, Lehéricy S, Hess EJ, Jinnah HA. The functional neuroanatomy of dystonia [Review]. Neurobiol Dis 2011; 42: 185–201.

Nisticò R, Pirritano D, Novellino F, Salsone M, Morelli M, Valentino P, et al. Blink reflex recovery cycle in patients with essential tremor associated with resting tremor. Neurology 2012a; 79: 1490–5.

Nisticò R, Pirritano D, Salsone M, Valentino P, Novellino F, Condino F, et al. Blink reflex recovery cycle in patients with dystonic tremor: a cross-sectional study. Neurology 2012b; 78: 1363–5.

Pal PK, Samii A, Schulzer M, Mak E, Tsui JK. Head tremor in cervical dystonia. Can J Neurol Sci 2000; 27: 137–42.

Papavassiliou E, Rau G, Heath S, Abosch A, Barbaro NM, Larson PS, et al. Thalamic deep brain stimulation for essential tremor: relation of lead location to outcome. Neurosurgery 2008; 62: 884–94.

Pinto AD, Lang AE, Chen R. The cerebellothalamocortical pathway in essential tremor. Neurology 2003; 60: 1985–7.

Prodoehl J, Yu H, Little DM, Abraham I, Vaillancourt DE. Region of interest template for the human basal ganglia: comparing EPI and standardized space approaches. Neuroimage 2008; 39: 956–65.

Prudente CN, Hess EJ, Jinnah HA. Dystonia as a network disorder: what is the role of the cerebellum? [Review]. Neuroscience 2014; 260: 23–35.

Raethjen J, Deuschl G. The oscillating central network of Essential tremor. Clin Neurophysiol 2012; 123: 61–4.

Roy A, Coombes SA, Chung JW, Archer DB, Okun MS, Hess CW, et al. Cortical dynamics within and between parietal and motor cortex in essential tremor. Mov Disord 2018; 34: 95–104.

Rubinov M, Sporns O. Complex network measures of brain connectivity: uses and interpretations. Neuroimage 2010; 52: 1059–69.

Shaikh AG, Jinnah HA, Tripp RM, Optican LM, Ramat S, Lenz FA, et al. Irregularity distinguishes limb tremor in cervical dystonia from essential tremor. J Neurol Neurosurg Psychiatry 2008; 79: 187–9.

Shaikh AG, Zee DS, Jinnah HA. Oscillatory head movements in cervical dystonia: Dystonia, tremor, or both? Mov Disord 2015; 30: 834–42.

Simonyan K, Ludlow CL. Abnormal activation of the primary somatosensory cortex in spasmodic dysphonia: an fMRI study. Cereb Cortex 2010; 20: 2749–59.

Simonyan K, Ludlow CL. Abnormal structure-function relationship in spasmodic dysphonia. Cereb Cortex 2012; 22: 417–25.

Vaillancourt DE, Haibach PS, Newell KM. Visual angle is the critical variable mediating gain-related effects in manual control. Exp Brain Res 2006; 173: 742–50.

Vaillancourt DE, Newell KM. Aging and the time and frequency structure of force output variability. J Appl Physiol 2003; 94: 903–12.

Vaillancourt DE, Slifkin AB, Newell KM. Intermittency in the visual control of force in Parkinson's disease. Exp Brain Res 2001; 138: 118–27.

Vidailhet M, Vercueil L, Houeto JL, Krystkowiak P, Benabid AL, Cornu P, et al. Bilateral deep-brain stimulation of the globus pallidus in primary generalized dystonia. N Engl J Med 2005; 352: 459–67.

Vo A, Sako W, Niethammer M, Carbon M, Bressman SB, Uluğ AM, et al. Thalamocortical connectivity correlates with phenotypic variability in dystonia. Cereb Cortex 2015; 25: 3086–94.